TISSUE ENGINEERING: Part C
Volume 19, Number 10, 2013

DOI: 10.1089/ten.tec.2012.0720

Methods Article

Optical Imaging Predicts Mechanical Properties During Decellularization of Cardiac Tissue

Nick Merna, MS,[1] Claire Robertson, MS,[1] Anh La,[1] and Steven C. George, MD, PhD[1–4]

Decellularization of xenogeneic hearts offers an acellular, naturally occurring, 3D scaffold that may aid in the development of an engineered human heart tissue. However, decellularization impacts the structural and mechanical properties of the extracellular matrix (ECM), which can strongly influence a cell response during recellularization. We hypothesized that multiphoton microscopy (MPM), combined with image correlation spectroscopy (ICS), could be used to characterize the structural and mechanical properties of the decellularized cardiac matrix in a noninvasive and nondestructive fashion. Whole porcine hearts were decellularized for 7 days by four different solutions of Trypsin and/or Triton. The compressive modulus of the cardiac ECM decreased to $<20\%$ of that of the native tissue in three of the four conditions (range 2–8 kPa); the modulus increased by $\sim 150\%$ (range 125–150 kPa) in tissues treated with Triton only. The collagen and elastin content decreased steadily over time for all four decellularization conditions. The ICS amplitude of second harmonic generation (SHG, A_{SHG}) collagen images increased in three of the four decellularization conditions characterized by a decrease in fiber density; the ICS amplitude was approximately constant in tissues treated with Triton only. The ICS ratio (R_{SHG}, skew) of collagen images increased significantly in the two conditions characterized by a loss of collagen crimping or undulations. The ICS ratio of two-photon fluorescence (TPF, R_{TPF}) elastin images decreased in three of the four conditions, but increased significantly in Triton-only treated tissue characterized by retention of densely packed elastin fibers. There were strong linear relationships between both the log of A_{SHG} ($R^2 = 0.86$) and R_{TPF} ($R^2 = 0.92$) with the compressive modulus. Using these variables, a linear model predicts the compressive modulus: $E = 73.9 \times \mathrm{Log}(A_{SHG}) + 70.1 \times R_{TPF} - 131$ ($R^2 = 0.94$). This suggests that the collagen content and elastin alignment determine the mechanical properties of the ECM. We conclude that MPM and ICS analysis is a noninvasive, nondestructive method to predict the mechanical properties of the decellularized cardiac ECM.

Introduction

Decellularization of xenogeneic hearts offers an instructive extracellular matrix (ECM) that may facilitate the development of engineered human heart tissue. The cardiac extracellular matrix (C-ECM) has been shown to promote functionality and viability of cardiomyocytes and mesenchymal stem cells, without eliciting an immune response upon implantation.[1,2] Additionally, the C-ECM potentially retains the physical and chemical cues to aid cells in proliferation and spatial reorganization.[1–3]

The decellularization process affects the ECM composition, structure, and mechanical properties,[4] which have been shown to affect the cell response upon reseeding. For example, the substrate stiffness significantly affects maturation and differentiation of immature ventricular myocytes.[5] In addition, cells cultured on 10 kPa collagen gels develop aligned sarcomeres, while cells cultured on gels with stiffness similar to the native myocardium (10–15 kPa) are more likely to beat, beat with a greater frequency, and generate a greater contractile force.[5–7] Furthermore, previous work has generally cultured cardiomyocytes on collagen-coated gels, which can mimic the stiffness of the native myocardium, but cannot replicate other structural features present in native tissue such as collagen crimping or undulations.[5,6] A network microstructure can impact the mechanical properties of the ECM.[8,9] Thus, retaining both the mechanical properties and structural features of the native myocardium will likely improve the performance of seeded cardiomyocytes during recellularization.

Imaging the collagen and elastin fibers of the C-ECM may improve our understanding of the relationship between mechanical properties and a cell response. Multiphoton microscopy (MPM) and image correlation spectroscopy (ICS) are an effective combination to noninvasively and nondestructively assess bulk mechanical properties of collagen

Departments of [1]Biomedical Engineering, [2]Chemical Engineering and Materials Science, and [3]Medicine, and [4]The Edwards Lifesciences Center for Advanced Cardiovascular Technology, University of California, Irvine, Irvine, California.

Table 1. Decellularization Conditions

Decell 3/4	0.02% Trypsin/0.05% EDTA/0.05% NaN_3 for 3 days and 3% Triton X-100/0.05% EDTA/0.05% NaN_3 for 4 days
Decell 1/6	0.02% Trypsin/0.05% EDTA/0.05% NaN_3 for 1 day and 3% Triton X-100/0.05% EDTA/0.05% NaN_3 for 6 days
Tryp only	0.02% Trypsin/0.05% EDTA/0.05% NaN_3 for 7 days
Trit only	3% Triton X-100/0.05% EDTA/0.05% NaN_3 for 7 days

hydrogels,[10–12] and may be useful for *in vivo* applications, including the assessment of elastin.[13] However, previous work has not considered additional structural features, such as collagen crimping, which is present in the natural ECM. It is not well understood how these structural features affect mechanical properties. The goal of the current work is to quantitatively and noninvasively characterize the impact of decellularization on the C-ECM microstructure and mechanical properties using MPM and ICS.

Materials and Methods

Preparation of C-ECM

Whole porcine hearts were obtained immediately after euthanasia of 40–55 kg, adult female Yorkshire pigs. The excess fat and connective tissue were removed, and the coronaries were perfused with phosphate-buffered saline to remove coagulated blood. Each heart was frozen at −80°C for at least 24 h to aid in cell lysis.[1] These hearts were then thawed at room temperature and decellularized over a 7-day period by coronary perfusion with four different solutions of either Trypsin/EDTA/NaN_3 and/or Triton/EDTA/NaN_3 (Table 1) as previously described.[1] All Trypsin conditions were at a concentration of 0.02%, and all Triton conditions were at a concentration of 3%. All solutions contained 0.05% EDTA and 0.05% $NaNa_3$. Different combinations of Trypsin and Triton were used as their mechanism of action should differentially impact the ECM.[1,14] Full-thickness left ventricular tissue samples (1×1 cm) were collected every 24 h for imaging of MPM of fiber ultrastructure, mechanical testing for compressive modulus and protein analysis of collagen, elastin, and DNA content.

Multiphoton microscopy

For MPM imaging, multiphoton excited autofluorescence (elastin) and second harmonic generation (SHG) (collagen) were measured (Zeiss LSM 510 Meta Microscopy System) at 5-μm intervals with depths ranging from 0 to 50 μm as previously described.[11] SHG arises from nonlinear interactions between the incident light and the noncentrosymmetric structure of the fibrillar collagen and, thus, uniquely reflects the fibrillar collagen for *in vitro* and *in vivo* samples.[15] Two-photon fluorescence (TPF) arises primarily from the autofluorescence of elastin.[16] Thus, MPM enables noninvasive visualization of collagen and elastin in intact, unstained tissues. The TPF and SHG signals were collected using a 40×/1.3 Achroplan oil-immersion objective. A circularly polarized Chameleon laser was focused on the C-ECM samples with a wavelength of 860 nm and an incident power ranging from 60–175 mW. The SHG collagen signal was obtained using a 390–465-nm bandpass filter. The TPF signal was collected simultaneously in a second channel, using a 500–550-nm bandpass filter. To maximize consistency, images from different days and from different animals were taken using the same set of optical parameters, such as gain and laser intensity.

Image correlation spectroscopy

ICS was performed on SHG and TPF images during decellularization to quantify image morphology using indices that reflect fiber alignment and fiber density. ICS employs autocorrelation of two-dimensional and spatially resolved data[11,17,18] to assess fiber orientation, alignment, size, and density.[11] MATLAB was first used to compute the two-dimensional spatial autocorrelation function (ACF) as previously described.[11] Briefly, the ACF was calculated by first multiplying the two-dimensional spatial fast Fourier transform (FFT) function of the image and its complex conjugate to get the power spectral density (PSD). The inverse FFT of the PSD produced the ACF. The central 32×32 pixel portion of the ACF was then cropped to remove the higher spatial lag. The cropped ACF was then fit to a two-dimensional Gaussian function, where σ_M and σ_m represented the standard deviation along the major and minor axis, respectively, R_{SHG} and R_{TPF} the ratios of σ_M and σ_m for SHG and TPF images, θ the orientation of the axis with respect to the horizontal, and A_{SHG} and A_{TPF} the peak amplitudes for SHG and TPF images, respectively (Fig. 1). Since we could not control the orientation of our image relative to a fixed structure feature in the heart, θ was not used

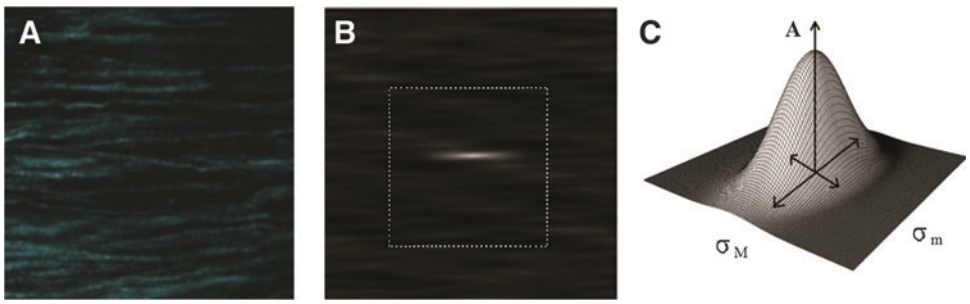

FIG. 1. Illustration of image correlation spectroscopy (ICS). **(A)** A second harmonic generation (SHG) image with collagen fibers oriented horizontally, **(B)** the autocorrelation function (ACF) of **(A, C)** the Gaussian fit of the centrally cropped ACF [dashed rectangle/square in **(B)**] with a wireframe representing the fit. *A* represents the peak amplitude, σ_M and σ_m represent the standard deviation along the major and minor axis. Color images available online at www.liebertpub.com/tec

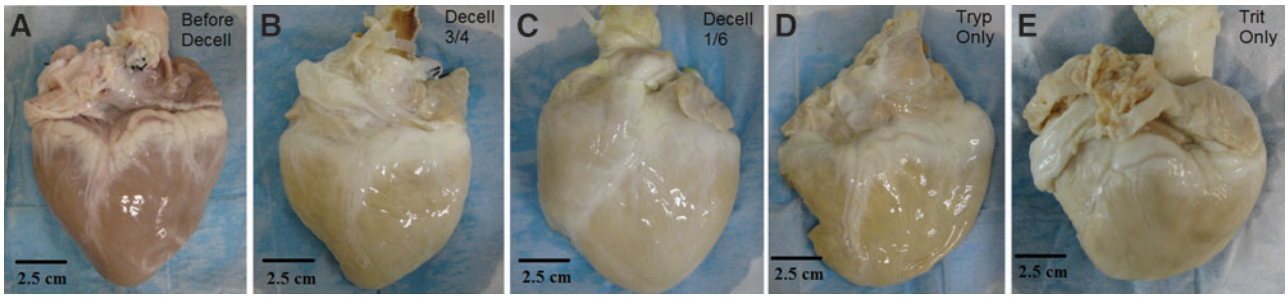

FIG. 2. Representative images of intact porcine hearts decellularized by coronary perfusion are shown **(A)** before decellularization, **(B)** after 0.02% Trypsin (Tryp) for 3 days and 3% Triton (Trit) X-100 for 4 days, **(C)** after 0.02% Trypsin for 1 day and 3% Triton X-100 for 6 days, **(D)** after 0.02% Trypsin for 7 days, and **(E)** after 3% Triton X-100 for 7 days. Color images available online at www.liebertpub.com/tec

in this study. A and R were used as indices that reflect the fiber density and alignment.[18]

Mechanical testing

The compressive modulus of the tissues was measured via indentation testing (Synergie 100; MTS Systems Corporation). The sample height ($\sim$15 mm) was measured using a linear extensor. Each sample was then compressed to 20% strain with a 5-mm radius plate at a rate of 0.02 mm/s. Data were acquired with a 10 N load cell at 50 Hz with a 12 bit data acquisition. The modulus was calculated in the linear region of the stress–strain curve. Each sample was tested in five locations and the values averaged.

Protein quantification

The total collagen, elastin, and DNA content per dry weight were assessed ($N=3$ for each time point) using commercially available kits (collagen: hydroxyproline assay kit Cedarlane, Elastin: Fastin assay kit Biocolor, DNA: Quant-iT PicoGreen dsDNA assay Invitrogen) following the manufacturer's instructions.

Statistical analysis

The SHG and TPF image parameters, compressive modulus, DNA content, collagen content, and elastin content were analyzed as a function of time during decellularization using one-way ANOVA. The compressive modulus was compared to A_{SHG}, A_{TPF}, R_{SHG}, and R_{TPF} using linear regression. In some cases, a log transformation was used to determine if a power law relationship between variables was evident. Logistic regression and the backward stepwise variable selection method using A and R from both SHG and TPF was applied to find the best model to predict the compressive modulus using the Akaike information criterion (AIC).[19] Multiple linear regression was then used to model the relationship between the variables, which had been selected by the AIC. SigmaStat was used to perform the statistical tests.

Results

Visual appearance and DNA content

All four decellularization conditions removed the red-brown coloration of the tissue by day 3. By day 7, the hearts from the four conditions were visually similar, displaying a whitish appearance (Fig. 2). Quantitative analysis of the DNA content of hearts decellularized by Trypsin/EDTA/NaN_3 for 3 days and Triton/EDTA/NaN_3 for 4 days (Decell 3/4), and hearts decellularized by Trypsin/EDTA/NaN_3 for 1 day and Triton/EDTA/NaN_3 for 6 days (Decell 1/6) showed (Table 2) a significant decrease in DNA compared to the DNA present in the nondecellularized samples (mean $\pm$ SD of 0.82 $\pm$ 0.18 and 0.75 $\pm$ 0.10, respectively, compared to 8.20 $\pm$ 0.61 ng DNA/mg sample). This represented a 90% and 91%, respectively, decrease in the amount of double-stranded DNA present in the tissue after decellularization. Tryp Only and Trit Only resulted in incomplete decellularization with DNA removal of $\sim$59% and 40%, respectively (mean $\pm$ SD of 3.39 $\pm$ 0.54 and 4.89 $\pm$ 0.37, respectively).

Mechanical properties, collagen, and elastin content

The compressive modulus of the nondecellularized porcine heart was 42.5 $\pm$ 14.4 kPa ($n=4$, mean $\pm$ SD). Decellularization progressively decreased the compressive modulus of the C-ECM to $<$20% of nondecellularized tissues in three of the four conditions (Fig. 3A). For Trit Only, the compressive modulus increased by $\sim$150% by day 3, and then remained constant. In contrast, the collagen content decreased steadily over time for all of the conditions (Fig. 3B), although Trit Only decreased the least ($\sim$40% compared to $\sim$ 80% for the other three conditions). The elastin content also decreased steadily over time for all four conditions (Fig. 3C). Again, Trit Only decreased the least ($\sim$30% compared to 50%–70%).

Collagen microstructure

The SHG images of the C-ECM demonstrated significant qualitative differences between the decellularization conditions (Fig. 4). Decell 3/4 and Tryp Only produced the C-ECM with straight and aligned collagen fibers. However, Decell 1/6 and Trit Only produced the C-ECM with crimped

Table 2. Extracellular Matrix DNA Quantification

Sample	*DNA (ng/mg dry weight)*
Native heart	8.20 $\pm$ 0.61
C-ECM (Decell 3/4)	0.82 $\pm$ 0.18
C-ECM (Decell 1/6)	0.75 $\pm$ 0.10
C-ECM (Tryp Only)	3.39 $\pm$ 0.54
C-ECM (Trit Only)	4.89 $\pm$ 0.37

C-ECM, cardiac extracellular matrix.

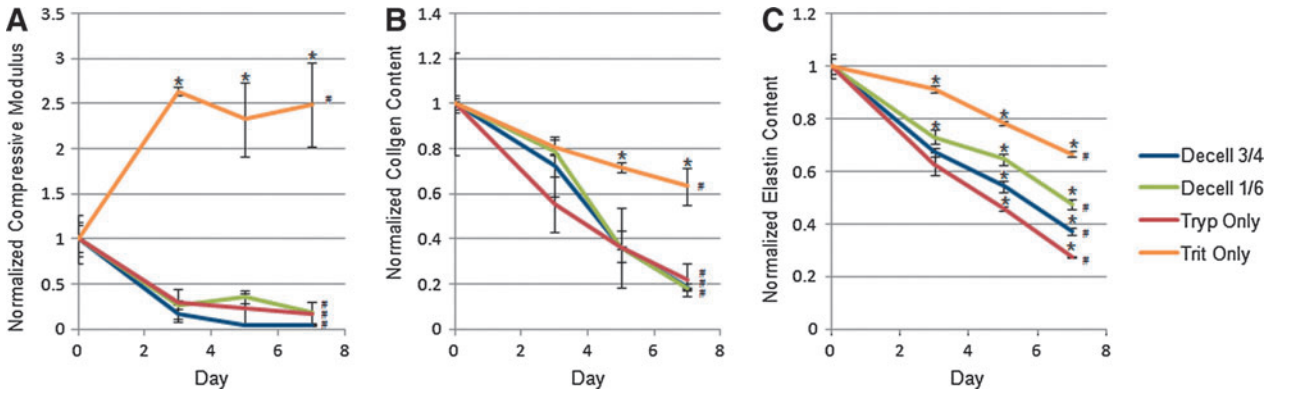

FIG. 3. The compressive modulus **(A)**, collagen content **(B)**, and elastin content **(C)** measured at days 0, 3, 5, and 7 of decellularization for all 4 decellularization conditions and normalized to day 0. The baseline compressive modulus for intact samples: 61.9, 31.5, 45.0, and 31.5 kPa. The baseline collagen content for intact samples: 465.6, 486.4, 503.3, and 505.3 μg/mg. The baseline elastin content for intact samples: 37.8, 37.7, 38.6, and 38.8 μg/mg. Asterisks represent statistically significant differences between conditions for that day ($^{*}p < 0.05$). Number signs represent statistical variation with time for that condition ($^{\#}p < 0.05$). Color images available online at www.liebertpub.com/tec

collagen fibers. These patterns began to emerge 3 days after initiation of the decellularization protocol.

Elastin microstructure

The elastin microstructure can be visualized from the TPF signal[16] (Fig. 5). There were marked qualitative differences between the decellularization conditions. Decell 3/4, Decell 1/6, and Tryp Only significantly disrupted the fine fiber architecture present in the native tissue. In contrast, the elastin structure was largely retained in Trit Only, but the fibers appeared more densely packed.

MPM and ICS analysis of collagen and elastin microstructure

ICS analysis of the SHG images demonstrated quantitative differences in the collagen microstructure among the

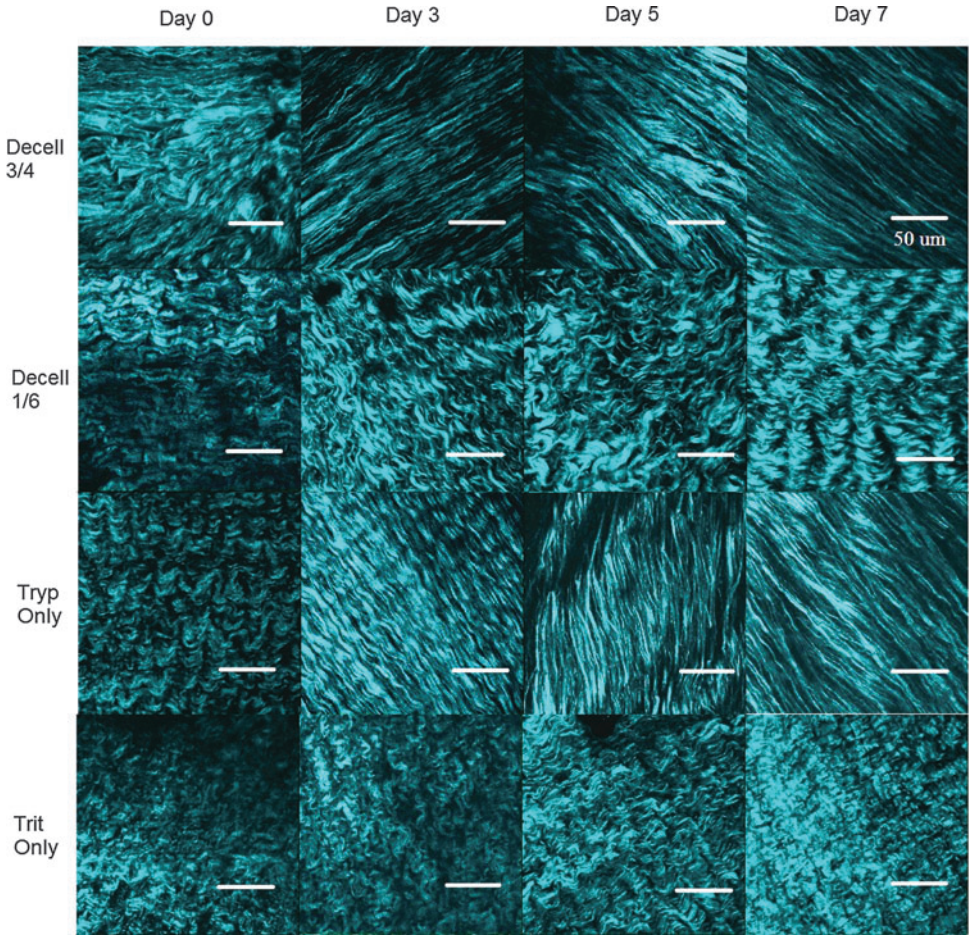

FIG. 4. Collagen microstructure. Representative SHG images reveal the fibrillar collagen microstructure of intact porcine hearts at days 0, 3, 5, and 7 for all four decellularization conditions. Images are 1024×1024 pixels and 230×230 μm. $N = 8$ images per condition were used for image analysis and statistics. Scale bar 50 μm. Color images available online at www.liebertpub.com/tec

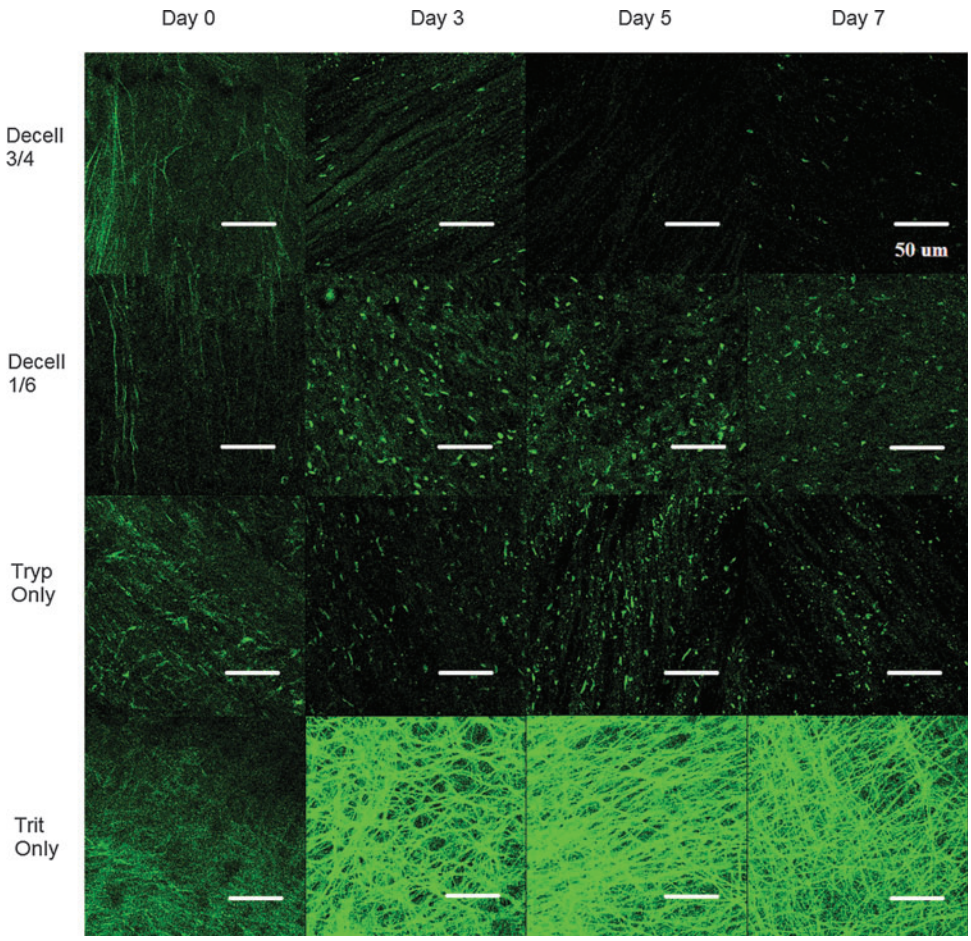

FIG. 5. Elastin microstructure. Representative two-photon fluorescence (TPF) images reveal the elastin microstructure of intact porcine hearts at days 0, 3, 5, and 7 for all four decellularization conditions. Images are 1024×1024 pixels and $230 \times 230\,\mu m$. $N = 8$ images per condition were used for image analysis and statistics. Scale bar $50\,\mu m$. Color images available online at www.liebertpub.com/tec

decellularization conditions (Fig. 6). A_{SHG} increased in three of the four decellularization protocols, the exception was Trit Only in which A_{SHG} was approximately constant (Fig. 6A). In contrast, the R_{SHG} increased significantly in the two conditions characterized by loss of collagen crimping (Decell 3/4 and Tryp Only). ICS analysis of the TPF images revealed quantitative differences in the elastin structure between the decellularization conditions: R_{TPF} decreased in Decell 3/4, Decell 1/6, and Tryp Only. In contrast, the R_{TPF} of Trit Only increased significantly characterized by retention of densely packed elastin fibers (Fig. 5).

Mechanical properties correlate with ICS amplitude and ratio

ICS image analysis of the C-ECM during the decellularization process was compared to direct mechanical testing and protein assays. A_{SHG} modestly correlated with the compressive modulus ($R^2 = 0.57$) and collagen content ($R^2 = 0.48$). However, there was a strong linear relationship between the log of A_{SHG} ($R^2 = 0.86$) and the log of the compressive modulus (Fig. 7A). R_{TPF} also strongly correlated with the compressive modulus ($R^2 = 0.92$). However, A_{TPF} ($R^2 = .13$) and R_{SHG} ($R^2 = 0.34$) showed little correlation with the compressive modulus.

Backward stepwise elimination based on AIC showed the best model to predict E contained two variables: A_{SHG} and R_{TPF} (AIC, 398). Thus, the best model to predict E was $E = 73.9 \times \mathrm{Log}(A_{SHG}) + 70.1 \times R_{TPF} - 131$. This model improved the fit to experimental data ($R^2 = 0.94$). In contrast, the AIC for the best single parameter model (R_{TPF}) was 418. Thus, by introducing one more variable (A_{SHG}), AIC improved by 20 (or 5%).

Discussion

Decellularization of the heart is a rapidly developing field that promises to create a scaffold for functional cardiac tissue engineering.[1,3,14] However, the decellularization process impacts the ECM, and a noninvasive, nondestructive method to assess the C-ECM, in particular, the mechanical properties, have not yet been presented. We have demonstrated that MPM (SHG from fibrillar collagen and TPF from elastin) imaging of the C-ECM and ICS analysis provides quantitative and objective information about the C-ECM in a noninvasive and nondestructive fashion that can predict the compressive modulus of the decellularized matrix.

Variability in microstructure/mechanics between decellularization conditions

It is perhaps important to first note that gross visual inspection of the C-ECM cannot distinguish between the decellularization protocols (Fig. 2). Thus, alternate methods are necessary to determine the extent of decellularization and changes to structural or mechanical properties. The most striking difference in the mechanical property among the

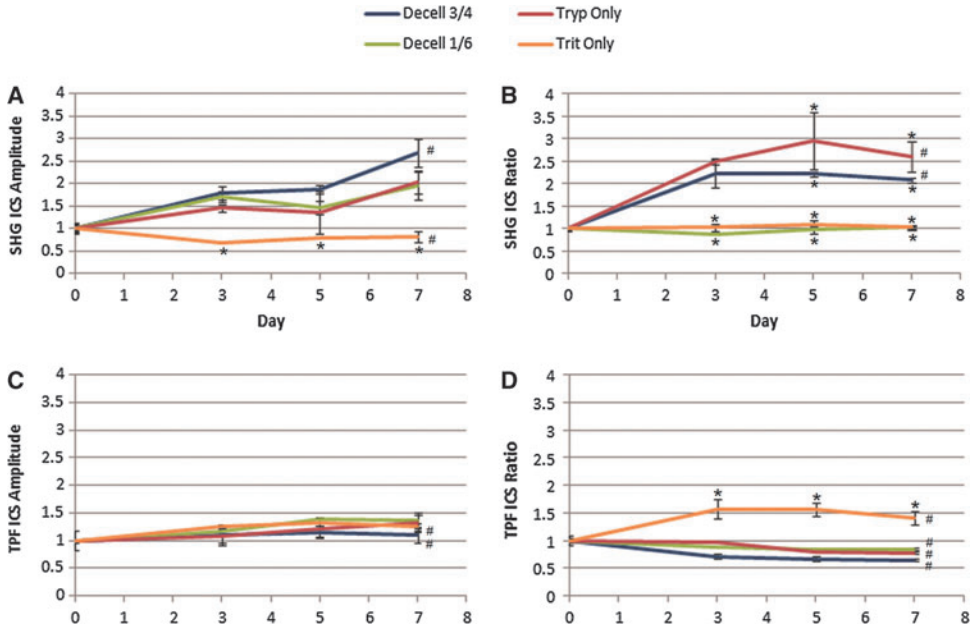

FIG. 6. ICS of SHG and TPF. **(A)** SHG ICS amplitude, **(B)** SHG ICS ratio, **(C)** TPF ICS amplitude, and **(D)** ICS ratio were calculated from SHG and TPF images of intact porcine hearts at days 0, 3, 5, and 7 for all four decellularization conditions and normalized to day 0. Baseline SHG ICS amplitude for intact samples were 0.12, 0.11, 0.15, and 0.13, respectively. The baseline SHG ICS ratio for intact samples were 1.50, 1.65, 1.23, and 1.23, respectively. Asterisks represent statistically significant differences between conditions for that day ($^{*}p < 0.05$). Number signs represent statistical variation with time for that condition ($^{\#}p < 0.05$). Color images available online at www.liebertpub.com/tec

decellularization conditions was the observation that Trit Only caused a significant increase in the compressive modulus, while the remaining three conditions all caused a significant decrease. There are several factors potentially responsible for this observation. Despite a decrease in the overall elastin content in all four conditions, TPF showed that Trit Only was the only condition to preserve the fibrillar nature of the elastin network (Fig. 5), although the density of the elastin fibers increased. The increased density of elastin could contribute to the increase in the compressive modulus. SHG also revealed a more densely crimped collagen structure of Trit Only, which could enhance the compressive modulus. This feature was reflected in the unique combination of a constant A_{SHG}, but an increase in R_{SHG}. Finally, the mechanism by which each reagent disrupts cells may also be a factor. Triton lyses cells by disrupting the cell membrane and, unlike Trypsin, did not break the cell–ECM bonds. This may result in significant cell residue (not DNA) that could impact the compressive modulus.

Despite the near complete removal of cellular DNA (comparable to previously published results),[1] Decell 1/6 preserved collagen crimping, a feature of the native ECM, while Decell 3/4 did not. The C-ECM with crimped collagen fibers had a twofold higher compressive modulus compared to the uncrimped C-ECM (5.8 kPa vs. 2.4 kPa, $p < 0.01$). These are physiologically relevant differences in the compressive modulus (between 1 and 15 kPa).[5,6] During embryonic development, the passive modulus of cardiac tissue is ~3–4 kPa and the modulus of tissue surrounding the myocardium ranges from 9–14 kPa.[20] The prolonged exposure to Trypsin likely disrupted the collagen and elastin protein fibrils leading to a loss of fiber density (Fig. 5).

While the C-ECM from Decell 3/4 and Decell 1/6 had different compressive moduli and collagen ultrastructure, they had similar levels of the collagen content. This suggests that the presence of crimping in the Decell 1/6 C-ECM may have been partly responsible for the higher compressive modulus. The increased compressive modulus of Trit Only and its preservation of elastin fibers (Fig. 5) also suggest that the presence of elastin may have played an important role in the mechanical properties in the C-ECM.

ICS amplitude and ICS ratio predict structure and mechanical properties

Previous work has shown that ICS parameters correlate with fiber properties such as width, density, and pore size.[11,17] However, additional properties, such as collagen crimping or elastin content, will likely affect bulk mechanical properties. Expanding ICS analysis to include these additional features will help further define the relationship between ICS and bulk mechanical properties in natural tissues.

In our study, A_{SHG} and R_{TPF} correlated well with the compressive modulus, and R_{SHG} appeared to increase with the loss of collagen crimping. Logistic regression and backward stepwise elimination based on AIC showed the best model to predict compressive modulus contained two variables (A_{SHG} and R_{TPF}), which improved the fit to experimental data ($R^2 = 0.94$) relative to a single variable (R_{TPF}). By introducing one more variable (A_{SHG}), AIC improved by 20 (or 5%). A_{TPF} ($R^2 = 0.13$) and R_{SHG} ($R^2 = 0.34$) showed almost no correlation with the compressive modulus and were therefore excluded from the model. The model's high degree of fit suggests

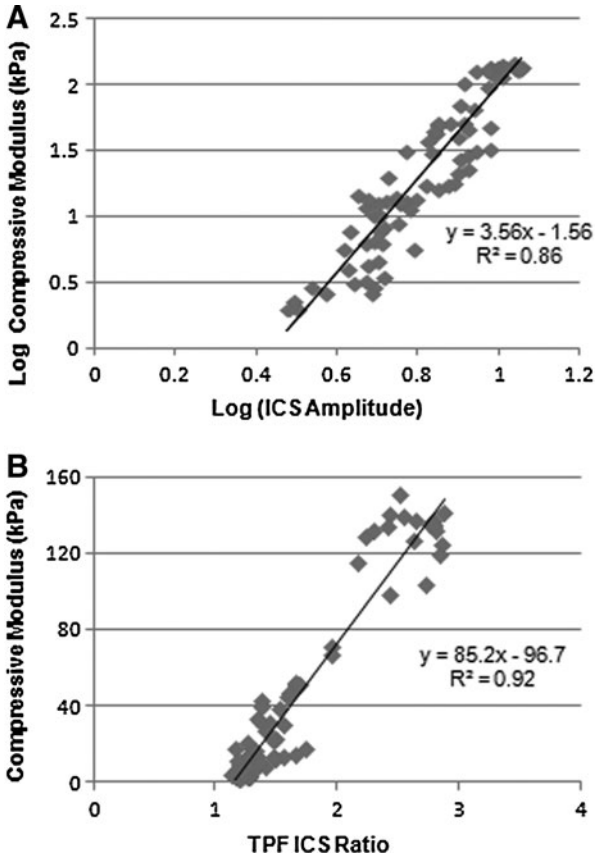

FIG. 7. The relationship between mechanical and optical properties. **(A)** The scaling relationship for the compressive modulus and ICS amplitude from SHG images and **(B)** the compressive modulus and ICS ratio from TPF images for all four decellularization conditions.

that MPM and ICS provide a noninvasive means to determine the structure and mechanical properties of the C-ECM.

The ICS amplitude has previously been shown to be inversely proportional to fiber density.[18] Thus, our observed increase in A_{SHG} and A_{TPF} is likely a result of decreased collagen and elastin fiber density, confirmed by the protein assays that demonstrated a loss of total collagen and elastin content. However, another factor is the presence of light scatterers, including cells, during the early stages of decellularization. Cells scatter photons and reduce the MPM signal.[15] Complete removal of cells results in sharper images of the SHG collagen structure and the TPF elastin structure. Thus, both loss of collagen and cells may have contributed to the observed increase in ICS amplitude.

Optimal decellularization for mechanical endpoints

Previous studies suggest an optimal ECM stiffness range for cardiomyocytes and cardiac fibroblast cell function exists.[5,6,21] Stiffness significantly affects maturation and differentiation of immature ventricular myocytes, development of aligned sarcomeres, and generation of contractile force.[5] Cardiomyocytes are also more likely to beat, and beat with greater frequency, when cultured on softer collagen gels with heart-like elasticity.[6,7] ECM mechanical properties also play a dominant role in maintaining fibroblast quiescence.[21] As artificial substrate stiffness increases from that of normal parenchymal tissue (~10 kPa) to that of fibrotic, collagen-rich tissue (35–70 kPa), cultured fibroblasts transition from quiescence to a state of increased proliferation and matrix synthesis, suggesting that controlling ECM stiffness promotes cell functionality.

Studies have recellularized the C-ECM using cardiac, endothelial, fibroblast, and stem cells, and have found that the scaffold's architecture and composition promote cell functionality. Recellularization of decellularized rat hearts with cardiac and endothelial cells, with subsequent electrical and mechanical stimulation, create contractile tissues.[3] Decellularized porcine hearts recellularized with cardiomyocytes support formation of organized cardiomyocyte sarcomeres,[1] and have been shown to beat and express typical cardiac cell markers within a few days of seeding.[2]

Despite the current success in recellularizing natural and artificial scaffolds, the effect of the collagen structure on cell fate remains relatively unexplored. A mechanical environment and structure similar to that of the native myocardium should be most favorable. When comparing our two decellularization conditions, Decell 1/6 produced a compressive modulus and structure more similar to the native ECM (42.4 kPa) relative to Decell 3/4 (5.8 kPa vs. 2.4 kPa). Additionally, Decell 3/4 appeared to damage the collagen structure and compromise mechanical integrity, as seen by the loss of crimping and decrease in fiber density. This suggests that Decell 1/6 would be the preferred decellularization condition for maintaining cell function. Tryp Only and Trit Only were not valid decellularization techniques, as DNA loss was incomplete. Nonetheless, these conditions provide information about the affect each individual reagent has on the collagen structure during the decellularization process. Trypsin severely reduced the structure and mechanical integrity, while Triton preserved the collagen crimping and increased the matrix stiffness. Our results emphasize the importance of appropriate timing when optimizing a decellularization protocol using these two reagents.

Conclusion

Decellularization of xenogeneic hearts potentially offers instructive matrix that may facilitate the development of engineered human heart tissue. Studies have shown that mechanical properties of the ECM can strongly influence the cell response; however, the decellularization process impacts the C-ECM structural and mechanical properties. We have presented a noninvasive, nondestructive method to assess the mechanical properties of the matrix that employs MPM imaging and ICS analysis. This process allows one to quantitatively assess the microstructure, and estimate the compressive modulus without compromising the C-ECM.

Acknowledgments

This work has been supported, in part, by a grant from the National Institutes of Health (R01 HL067954 to SCG), as well as the Laser Microbeam and Medical Program (LAMMP) at the Beckman Laser Institute. The LAMMP facility is supported by the National Institutes of Health (NIH P41 EB015890). We would also like to recognize the assistance

and expertise of Dr. Tatiana Krasieva at the Beckman Laser Institute for MPM imaging, and Mr. Earl Steward for assistance in procuring the porcine hearts.

Disclosure Statement

No competing financial interests exist.

References

1. Wainwright, J.M., Czajka, C.A., Patel, U.B., Freytes, D.O., Tobita, K., Gilbert, T.W., and Badylak, S.F. Preparation of cardiac extracellular matrix from an intact porcine heart. Tissue Eng Part C Methods **16,** 525, 2010.
2. Eitan, Y., Sarig, U., Dahan, N., and Machluf, M. Acellular cardiac extracellular matrix as a scaffold for tissue engineering: *in vitro* cell support, remodeling, and biocompatibility. Tissue Eng Part C Methods **16,** 671, 2010.
3. Ott, H.C., Matthiesen, T.S., Goh, S.K., Black, L.D., Kren, S.M., Netoff, T.I., and Taylor, D.A. Perfusion-decellularized matrix: using nature's platform to engineer a bioartificial heart. Nat Med **14,** 213, 2008.
4. Payam Akhyari, H.A., Patricia gwanmesia, mareike barth, stefanie hoffmann, jorn huelsmann, karlheinz preuss, artur lichtenberg. the quest for an optimized protocol for whole-heart decellularization: a comparison of three popular and a novel decellularization technique and their diverse effects on crucial extracellular matrix qualities. Tissue Eng Part C **17,** 11, 2011.
5. Jacot, J.G., Kita-Matsuo, H., Wei, K.A., Chen, H.S., Omens, J.H., Mercola, M., and McCulloch, A.D. Cardiac myocyte force development during differentiation and maturation. Ann N Y Acad Sci **1188,** 121, 2010.
6. Engler, A.J., Carag-Krieger, C., Johnson, C.P., Raab, M., Tang, H.Y., Speicher, D.W., Sanger, J.W., Sanger, J.M., and Discher, D.E. Embryonic cardiomyocytes beat best on a matrix with heart-like elasticity: scar-like rigidity inhibits beating. J Cell Sci **121,** 3794, 2008.
7. Shapira-Schweitzer, K., and Seliktar, D. Matrix stiffness affects spontaneous contraction of cardiomyocytes cultured within a PEGylated fibrinogen biomaterial. Acta Biomater **3,** 33, 2007.
8. Hiltner, A., Cassidy, J.J., and Baer, E. Mechanical Properties of Biological Polymers. Annu Rev Mater Sci **15,** 455, 1985.
9. Maria Comninou, I.V.Y. Dependence of stress-strain nonlinearity of connective tissue on the geometry of collagen fibers. J Biomechanics **9,** 6, 1976.
10. Raub, C.B., Putnam, A.J., Tromberg, B.J., and George, S.C. Predicting bulk mechanical properties of cellularized collagen gels using multiphoton microscopy. Acta Biomater **6,** 4657, 2010.
11. Raub, C.B., Unruh, J., Suresh, V., Krasieva, T., Lindmo, T., Gratton, E., Tromberg, B.J., and George, S.C. Image correlation spectroscopy of multiphoton images correlates with collagen mechanical properties. Biophys J **94,** 2361, 2008.
12. Raub, C.B., Suresh, V., Krasieva, T., Lyubovitsky, J., Mih, J.D., Putnam, A.J., Tromberg, B.J., and George, S.C. Noninvasive assessment of collagen gel microstructure and mechanics using multiphoton microscopy. Biophy J **92,** 10, 2007.
13. Raub, C.B., Mahon, S., Narula, N., Tromberg, B.J., Brenner, M., and George, S.C. Linking optics and mechanics in an *in vivo* model of airway fibrosis and epithelial injury. J Biomed Opt **15,** 015004, 2010.
14. Badylak, S.F., Taylor, D., and Uygun, K. Whole-organ tissue engineering: decellularization and recellularization of three-dimensional matrix scaffolds. Annu Rev Biomed Eng **13,** 27, 2011.
15. Zoumi, A., Yeh, A., and Tromberg, B.J. Imaging cells and extracellular matrix *in vivo* by using second-harmonic generation and two-photon excited fluorescence. Proc Natl Acad Sci U S A **99,** 11014, 2002.
16. Richards-Kortum, R., and Sevick-Muraca, E. Quantitative optical spectroscopy for tissue diagnosis. Annu Rev Phys Chem **47,** 555, 1996.
17. Robertson, C., and George, S.C. Theory and practical recommendations for autocorrelation-based image correlation spectroscopy. J Biomed Opt **17,** 080801, 2012.
18. Mir, S.M., Baggett, B., and Utzinger, U. The efficacy of image correlation spectroscopy for characterization of the extracellular matrix. Biomed Opt Expr **3,** 215, 2012.
19. Akaike, H., Amari, S., Kitagawa, G., Kabashima, S., and Simodaira, H. Akaike information criterion. Math Sci (Tokyo) **14,** 5, 1976.
20. Berry, M.F., Engler, A.J., Woo, Y.J., Pirolli, T.J., Bish, L.T., Jayasankar, V., Morine, K.J., Gardner, T.J., Discher, D.E., and Sweeney, H.L. Mesenchymal stem cell injection after myocardial infarction improves myocardial compliance. Am J Physiol Heart Circ Physiol **290,** H2196, 2006.
21. Liu, F., Mih, J.D., Shea, B.S., Kho, A.T., Sharif, A.S., Tager, A.M., and Tschumperlin, D.J. Feedback amplification of fibrosis through matrix stiffening and COX-2 suppression. J Cell Biol **190,** 693, 2010.

Address correspondence to:
Steven C. George, MD, PhD
Department of Biomedical Engineering
University of California, Irvine
2420 Engineering Hall
Irvine, CA 92697-2715

E-mail: scgeorge@uci.edu

Received: December 5, 2012
Accepted: February 19, 2013
Online Publication Date: May 1, 2013